Ab initio study of generalized collective excitations in molten NaI

Taras Bryk and Ihor Mryglod
Institute for Condensed Matter Physics, National Academy of Sciences of Ukraine, 1 Svientsitskii Street, UA-79011 Lviv, Ukraine
and Institute of Applied Mathematics and Fundamental Sciences, Lviv Polytechnic National University, UA-79013 Lviv, Ukraine
(Received 30 August 2008; published 21 May 2009)

A combination of *ab initio* molecular dynamics and parameter-free analysis of time-correlation functions based on the generalized collective mode approach is applied for the study of collective dynamics in a molten salt NaI beyond the hydrodynamic region and manifestation of collective excitations in dynamic structure factors. The dispersion and damping of acoustic and optic modes as well as the wave-number dependence of relaxation processes are discussed. Contributions from opticlike modes to the total and concentration dynamic structure factors are estimated. Analysis of the inelastic x-ray scattering (IXS)-weighted total dynamic structure factor at $T=953$ K is performed in order to verify the possibility of direct observation of optic modes in molten NaI in the IXS experiments.

DOI: 10.1103/PhysRevB.79.184206 PACS number(s): 61.20.Ja, 61.20.Lc, 62.60.+v

I. INTRODUCTION

Computer simulations of time-dependent correlations in liquids represent a powerful tool for exploring single-particle and collective dynamics. The density-density time-correlation functions obtained directly in molecular-dynamics (MD) simulations can be compared via the time Fourier transform with the experimental intensities $I(k,\omega) \sim S(k,\omega)$ (k and ω are the wave number and frequency, respectively), measured in quasielastic neutron or x-ray scattering experiments[1] and known as the dynamical structure factors. In order to understand which microscopic processes are responsible for the shape of $S(k,\omega)$ in different regions of the (k,ω) plane corresponding to distinct spatial and time scales, one has to perform a theoretical analysis of MD-derived time-correlation functions $F_{ij}(k,t)$ or their time Fourier transforms by appropriate theoretical models. The simplest theoretical model for analysis is the hydrodynamic one, which is applicable, however, only for sufficiently small wave numbers and frequencies, i.e., on the spatial and time scales, when the atomic structure is indistinguishable and liquid is treated as continuum. Usually the wave numbers k accessible in the neutron and x-ray scattering experiments are located beyond the hydrodynamic region, i.e., in the region where short-time processes on molecular scale (we will call them throughout this paper as *kinetic* processes) play an important role and hydrodynamic models require a generalization. Without a proper theoretical analysis based on generalized models one can make potentially wrong conclusions about the dispersion law of collective excitations and their contributions to the shape of partial dynamic structure factors $S_{ij}(k,\omega)$ of many-component liquids.

The widely used estimation of dispersion law of acoustic excitations from analysis of peak positions of Fourier-transformed density-density time-correlation functions, obtained in molecular-dynamics simulations of liquids, itself is not a unique procedure. The intuitive definition of the frequency of collective excitation via the side peak locations of $S_{ij}(k,\omega)$ or $C_{ij}^{L}(k,\omega)$ is supported by the analytical expressions only in the limit $k\to 0$. For wave numbers beyond the hydrodynamic region the peak positions of dynamical structure factors $S_{ij}(k,\omega)$ and longitudinal current spectral function,

$$C_{ij}^{L}(k,\omega) = \frac{\omega^2}{k^2} S_{ij}(k,\omega), \tag{1}$$

are different although it is clear that both spectral functions reflect the manifestation of the same collective excitations. A well-defined side peak with location $\omega=\omega_s(k)$ of the dynamical structure factor is shifted up approximately by $\Gamma_s^2(k)/\omega_s$, when it is estimated from the spectral function $C_{ij}^{L}(k,\omega)$. Here $\Gamma_s(k)$ is the half width at half height of the Brillouin peak and corresponds to the damping coefficient of acoustic excitations. Hence, the numerical estimation of dispersion laws from the peak positions of $C_{ij}^{L}(k,\omega)$ does not correspond to real dispersion law of collective excitations. Only a correct theoretical analysis of MD-derived time-correlation functions or corresponding spectral functions can result in the true dispersion of collective excitations. It is obvious from Eq. (1) that a theoretical scheme, based on the definition of collective excitations as the poles of spectral functions, which is the generally accepted definition in statistical physics, will result in identical dispersion laws from $S_{ij}(k,\omega)$ and $C_{ij}^{L}(k,\omega)$. For the case of binary liquids that definition of collective excitations was successfully applied within the viscoelastic approximation of the memory function formalism.[2,3]

Theoretical studies of dispersion curves of collective excitations are strongly dependent on the theoretical model applied. For the case of molten salts the most simple model is based on rigid-ion (RI) treatment, which neglects any polarization effects of the ions.[4] More correct approach based on effective pair interactions between ions with a massless shell, which reflects the polarization effects of localized electron clouds, was used for studies of collective excitations in molten NaI in Refs. 5 and 6. Classical molecular-dynamics simulations were performed also on molten NaI using a rigid-ion potential to which the induced dipole polarization of the anions was added. The polarization was added in such a way that point dipoles were induced on the anions by both local

electric field and short-range damping interactions that oppose the electrically induced dipole moments.[7] Recently it became possible to apply the *ab initio* (AI) simulations in the studies of structural and dynamical properties of molten salts.[8] The advantage of the *ab initio* simulations over classical MD of molten salts within the core-shell model is in more correct reproduction of polarization effects because *ab initio* simulations are free of any constraints on ionic charge. However, there were no attempts to estimate dispersion of collective excitation in molten NaI even from peak positions of relevant current spectral functions obtained in the first-principle simulations. Precise *ab initio* calculations of the dispersion curves and damping of collective excitations are absent in the literature, while for the case of crystals the precise estimation of dispersion curves from *ab initio* simulations is actively elaborated.[9] For the case of liquids, especially liquid metals and ionic systems, there is a need in development of theoretical methods, which in combination with the *ab initio* molecular dynamics would provide correct estimation of the dispersion and the damping of collective excitations. Therefore, an *ab initio* study, based on consistent theoretical approach and focused on collective excitations in a molten salt is of great interest for understanding general features of spectra formation in molten salts.

In this paper we report the generalized collective mode (GCM) study of longitudinal and transverse dynamics of a molten salt NaI with the main attention focused on the dispersion of collective excitations, and opticlike (charge) waves in particular. We will obtain the dispersion relations numerically in a general scheme taking into account main local (with the same wave number) coupling effects between the slow (hydrodynamic) and faster processes, i.e., we will take into account all possible damping mechanisms of collective excitations. Recently the interest on the collective dynamics in molten salts was revived by the inelastic x-ray scattering (IXS) experiments performed on molten NaI at 953 K,[10] and the reported direct observation of opticlike excitations on the shape of total dynamical structure factor. These experimental findings are especially interesting because the opticlike excitations belong to a wide class of nonhydrodynamic processes in liquids. The general theory of nonhydrodynamic modes[11,12] and of the opticlike excitations in particular[13,14] states that the contributions from nonhydrodynamic collective processes to the total dynamical structure factor vanish in the long-wavelength limit. Therefore, the parameter-free studies on prediction of frequency window for observation of opticlike excitations and estimation of their contributions to the dynamical structure factors are very important. We aimed to estimate in this study the contributions from the acoustic and optic excitations to different spectral functions including the x-ray weighted total dynamical structure factors in molten NaI at 953 K in order to shed light on the issue of whether it was possible to observe the long-wavelength opticlike excitations in the IXS experiments.[10] In order to take correctly into account all the polarization effects in the molten salt and predict the correct frequency window of frequencies corresponding to opticlike excitations, we applied in this study the *ab initio* molecular-dynamics simulations. The parameter-free GCM approach,[12,15] which to date is the most reliable method of analysis of time-correlation functions relevant to collective dynamics in liquids, is applied for estimation of the dispersion and the damping of longitudinal and transverse collective modes in the wide region of wave numbers.

The remaining part of the paper is organized as follows. In Sec. II we shortly describe the GCM approach for the study of generalized collective excitations in liquids and give all the details of MD simulations. Section III contains an analysis of collective dynamics in molten NaI based on a six-variable viscoelastic GCM approach. An analysis of the x-ray weighted dynamic structure factor will be performed with the purpose of reproducing the experimentally measured $S_{\mathrm{IXS}}(k,\omega)$, and Sec. IV contains conclusions of this study.

II. METHOD

A. Generalized collective modes approach

Within the GCM approach one has to solve the generalized Langevin equation in matrix form in terms of dynamical collective eigenmodes of the liquid system. In fact it is a parameter-free analysis of MD-derived time-correlation functions by estimating dynamical collective eigenmodes in the liquid as the eigensolutions of the generalized hydrodynamic matrix $\mathbf{T}(k)$, defined in Markovian approximation as follows;[15]

$$\mathbf{T}(k) = \mathbf{F}(k,t=0)\tilde{\mathbf{F}}^{-1}(k,z=0), \tag{2}$$

where $\mathbf{F}(k,t)$ is the matrix of time-correlation functions $F_{ij}(k,t)=\langle A_i(k,0)A_j^*(k,t)\rangle$ constructed on a chosen basis set of N_v dynamical variables $\mathbf{A}^{(N_v)}(k,t)$, and $\tilde{\mathbf{F}}(k,z)$ is its Laplace transform. The most general basis set of dynamical variables consists of the hydrodynamic variables and their time derivatives, which being orthogonal to the hydrodynamic variables are supposed to describe correctly short-time processes in liquids. The time evolution of all dynamical variables can be obtained in MD simulations with the purpose of parameter-free estimation of the elements of matrix $\mathbf{F}(k,t)$. All the extended (nonhydrodynamic) dynamical variables usually are generated as the nth time derivative of partial currents, and can be obtained in analytical form and simply calculated from the MD data. The complex-conjugated pairs of eigenvalues of $\mathbf{T}(k)$, which correspond to propagating processes, estimated at different wave numbers formed the spectra of collective excitations.

Within the GCM approach one reconstructs the time-correlation functions, called as the GCM replica, in separable form:

$$F_{ij}^{(N_v)}(k,t) = \sum_{\alpha=1}^{N_v} G_{ij}^{\alpha}(k)e^{-z_{\alpha}(k)t}, \tag{3}$$

where each term corresponds to a separated contribution from the collective mode $z_{\alpha}(k)$ with a complex weight $G_{ij}^{\alpha}(k)$.

In this study we use for theoretical analysis of longitudinal dynamics in molten NaI an extended set of six dynamical variables

$$\mathbf{A}^{(6)}(k,t) = \{n_\alpha(k,t), n_\beta(k,t), J^L_\alpha(k,t), J^L_\beta(k,t), \dot{J}^L_\alpha(k,t), \dot{J}^L_\beta(k,t)\}, \tag{4}$$

composed of partial densities, partial currents, and their time derivatives (extended dynamic variables). The overdots in Eq. (4) mean the first time derivatives of corresponding dynamical variables. One can use here either a "partial" representation of the dynamical variables, α,β=Na,I, or one that is more correct from the point of view of conserved quantities of the system—a "mass-concentration" (*M*-*X*) representation $\alpha,\beta=m,x$,[16] where instead of partial dynamical variables one has to consider their linear combinations, which represent: the total mass-density $n_m(k,t)$, mass-concentration density $n_x(k,t)$, corresponding longitudinal components of the total and mass-concentration currents, and their first time derivatives.[14] It is obvious that the eigenvalues of the generalized hydrodynamic matrix will be identical independently on the chosen "partial" or "mass-concentration" representation of the dynamical variables in $\mathbf{A}^{(6)}(k,t)$ because they are connected by a linear transformation. The partial densities

$$n_\alpha(k,t) = \frac{1}{\sqrt{N}} \sum_{i=1}^{N_\alpha} e^{i\mathbf{k}\mathbf{r}_{i,\alpha}(t)}, \quad \alpha = \mathrm{Na,I}, \tag{5}$$

and partial mass currents

$$\mathbf{J}_\alpha(k,t) = \frac{1}{\sqrt{N}} \sum_{i=1}^{N_\alpha} m_\alpha \mathbf{v}_{i,\alpha}(t) e^{i\mathbf{k}\mathbf{r}_{i,\alpha}(t)}, \quad \alpha = \mathrm{Na,I}, \tag{6}$$

are the dynamical variables, which are most easily sampled in MD simulations. In Eqs. (5) and (6) the $\mathbf{r}_{i,\alpha}(t)$ and $\mathbf{v}_{i,\alpha}(t)$ are the position and velocity of particles, and m_α and N_α are the mass and number of particles of αth kind.

Since there are some known analytical results for the long-wavelength limit of the "total number-concentration" (*T*-*C*) Bhatia-Thornton static and dynamic structure factors,[16] below we will use some static structure factors and time-correlation functions obtained on the (*T*-*C*) densities:

$$n_t(k,t) = n_{\mathrm{Na}}(k,t) + n_{\mathrm{I}}(k,t),$$

$$n_c(k,t) = \frac{1}{2}[n_{\mathrm{Na}}(k,t) - n_{\mathrm{I}}(k,t)] \equiv \frac{\bar{m}^2}{m_{\mathrm{Na}} m_{\mathrm{I}}} n_x(k,t). \tag{7}$$

Note that the mass-concentration density $n_x(k,t)$ is simply proportional by a constant to the concentration density $n_c(k,t)$, and the mass concentration is defined as $x_\alpha = m_\alpha N_\alpha / M$, where $M = m_{\mathrm{Na}} N_{\mathrm{Na}} + m_{\mathrm{I}} N_{\mathrm{I}} = \bar{m} N$.

The transverse dynamics is studied within the same level of approximation with respect to treatment of short-time processes, as it is for the longitudinal dynamics, i.e., restricting the extended variables by the first time derivatives of relevant currents:

$$\mathbf{A}^{(4T)}(k,t) = \{J^T_\alpha(k,t), J^T_\beta(k,t), \dot{J}^T_\alpha(k,t), \dot{J}^T_\beta(k,t)\}. \tag{8}$$

Another dynamical model is closely connected with the collective propagating excitations described by the viscoelastic dynamical model [Eq. (4)]. Yet in the 1980s it was realized that the dispersion of acoustic and optic excitations in binary metallic glasses approximately can be obtained from a diagonalized matrix of the second frequency moments of the current spectral functions $C^{L,T}_{\alpha\beta}(k,\omega)$.[17] This intuitive approach was supported by recent analytical results for dispersion of "bare" collective modes $\omega^0_i(k)$.[18] They were obtained when in the viscoelastic dynamical model [Eq. (4)] one neglected the coupling to slow density fluctuations, and remaining effective four-variable model,

$$\mathbf{A}^{(4)}(k,t) = \{J^L_\alpha(k,t), J^L_\beta(k,t), \dot{J}^L_\alpha(k,t), \dot{J}^L_\beta(k,t)\}, \tag{9}$$

described collective modes without any damping with dispersion in complete agreement with the results in Ref. 17.

B. Details of *ab initio* molecular-dynamics simulations

Time-correlation functions for molten NaI were obtained from the *ab initio* molecular dynamics on Born-Oppenheimer surface (VASP package). A system of 150 particles was simulated in constant volume and temperature (NVT) ensemble using a cubic box under periodic boundary conditions. Two thermodynamic points were simulated: at experimental temperature of 953 K (Ref. 10) and at T =1080 K, which was the subject of the rigid-ion study in Ref. 19.

The electron-ion interactions were represented by the Kresse-Hafner ultrasoft pseudopotentials[20] and the highest default cutoff energy for them of 122.17 eV was used. Additional tests of total-energy convergence with cutoff of 165 and 190 eV were performed in order to check the reliability of the chosen cutoff energy. We have used the generalized gradient approximation for energy functional in Perdew-Wang-91 formulation.[21] In the actual simulations the electronic density was constructed using a single Γ point in the Brillouin zone and the time step was 1.5 fs.

For each thermodynamic point the length of production run was of 50 000 time steps in order to obtain reliable convergence of static and time-correlation functions needed for the subsequent GCM analysis. Thirty k points were sampled with the smallest wave numbers of $k_{\min}$=0.329 Å^{-1} for T =953 K and $k_{\min}$=0.326 Å^{-1} for T=1080 K. For each k point we analyzed the MD-derived time-correlation functions by the GCM approach, calculated the spectra of longitudinal and transverse collective excitations, and estimated mode contributions to the shape of dynamic structure factors using the well tested dynamic models.[13,14]

Since to date there does not exist a scheme for sampling of the heat fluctuations in *ab initio* molecular dynamics of liquids, we performed additional classical molecular-dynamics calculations for the molten NaI in order to make estimates for the ratio of the specific heats, which according to hydrodynamics defines the coupling between density and heat fluctuations. We have performed classical MD simulations of molten NaI in microcanonical ensemble with 1000 particles over 300 000 time steps of 2 fs in order to obtain well-converged generalized thermodynamic quantities, including the generalized ratio of specific heats. Each sixth configuration was taken for calculations of corresponding static averages and time-correlation functions. The param-

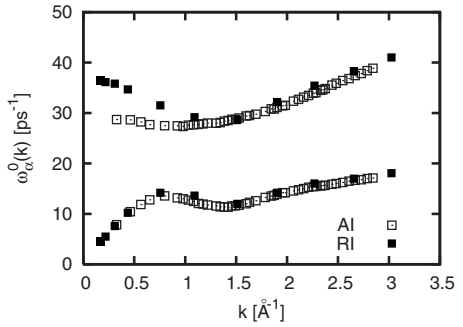

FIG. 1. Correspondence of the bare frequencies for molten NaI, obtained from classical RI and AI simulations.

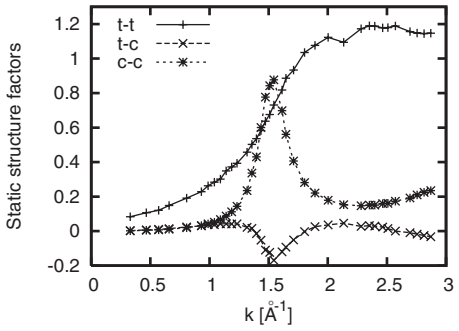

FIG. 2. Bhatia-Thornton static structure factors, directly evaluated in *ab initio* molecular dynamics: density-density $S_{tt}(k)$, concentration-concentration $S_{cc}(k)$, and density concentration $S_{tc}(k)$ at 1080 K.

eters of Tosi-Fumi potentials for rigid-ion classical simulations of NaI were taken from the Ref. 22.

In order to check whether there is sense in using some information about heat fluctuations sampled in classical MD simulations, and whether the periodic boundary conditions for two different in size systems studied by *ab initio* and classical molecular dynamics affected the obtained results, we have compared some quantities from both simulations. We have calculated the diagonalized second frequency moments of the current-current spectral functions $C_{ij}(k,\omega)$ following Ref. 17, which have the sense of square of "bare" frequencies. The second frequency moments essentially depend on the forces acting on ions. In Fig. 1 we show the bare frequencies $\omega^0_\alpha(k)$, obtained from the RI classical simulations and from ab initio molecular dynamics (AI MD). A striking agreement for bare modes from both simulations is observed for low-frequency modes. A "softening" of the high-frequency modes in the long-wavelength region, obtained from the *ab initio* simulations, is the consequence of polarization of electron density, similar as it was estimated in the *ab initio* study of collective dynamics of molten NaCl.[18] In general, the good correspondence of bare frequencies from classical and *ab initio* simulations can be an evidence of negligible size effects.

The static averages in the classical and *ab initio* simulations were well converged due to large number of configurations taken in calculations of the averages. The uncertainty of the static quantities was not larger than 3–4 %. Dynamic quantities, needed for the GCM analysis, such as correlation times[15] were estimated from the corresponding time-correlation functions and their uncertainty was not larger than 7%. The eigenvalues obtained numerically in the GCM approach are very sensitive to uncertainties in static and dynamic quantities—in case of poorly converged static or dynamic input quantities, one would obtain negative real parts of eigenvalues, i.e., nonphysical result. For both temperatures studied here we have obtained smooth wave-number dependence of the eigenvalues of generalized hydrodynamic matrix, reported below, which is another evidence of the high precision of performed calculations.

III. RESULTS AND DISCUSSION

A. Static quantities

Static properties of molten NaI have been studied already in the *ab initio* molecular dynamics;[8] therefore here we present only some calculated static properties needed in the subsequent analysis of collective excitations and their contributions to the dynamical structure factors. The most correct representation of atomic collective dynamics in molten salts from *ab initio* molecular dynamics is in terms of *T-C* or *M-X* sets of dynamical variables because in contrast to classical rigid-ion models the explicit treatment of charge fluctuations in the *ab initio* approach is too complicated. In Fig. 2 three main Bhatia-Thornton static structure factors are shown for molten NaI at 1080 K: $S_{tt}(k)$, $S_{tc}(k)$, and $S_{cc}(k)$ correspond to the "total density-total density," "total density-concentration density," and "concentration density-concentration density" structure factors, respectively. The structure factors at 953 K are very similar to the ones at 1080 K. For the analysis of dispersion of collective excitations the following features of the static structure factors are rather important: very sharp first peak of the concentration-concentration structure factor is located at $k \sim 1.51$ Å^{-1} and there is the absence of the pronounced first peak on the shape of $S_{tt}(k)$ (Fig. 2). Concerning the long-wavelength region, we are mainly interested in the long-wavelength asymptote of $S_{cc}(k)$ that should be proportional to k^2.[23] Comparing the long-wavelength asymptotes of $S_{cc}(k)$ obtained within the classical rigid-ion simulations and from *ab initio* MD, one can estimate the value of high-frequency dielectric permittivity ε, which describes effects of bare charge screening due to electron shell deformability. The estimated value of $\varepsilon=3.59$ for molten NaI is in agreement with the high-frequency dielectric permittivity of NaI crystals $\varepsilon_\infty=3.01$.[4] One can expect to obtain closer agreement with the experimental value of ε_∞ by using larger number of particles in the simulations of molten NaI because as it was shown in Ref. 24 the region of wave numbers with the hydrodynamic asymptotes of static and dynamic quantities reduces with increasing the mass ratio of components $m_{\text{heavy}}/m_{\text{light}}$ in binary melts.

Other important static quantities, which can be used for analysis of collective dynamics in molten salts, are the generalized wave-number-dependent thermodynamic quantities such as the generalized ratio of specific heats $\gamma(k)$ or the generalized linear thermal-expansion coefficient $\alpha_T(k)$. Since huge efforts are needed for calculations of energy fluctuations in *ab initio* molecular dynamics, we report here the generalized thermodynamic quantities obtained in classical

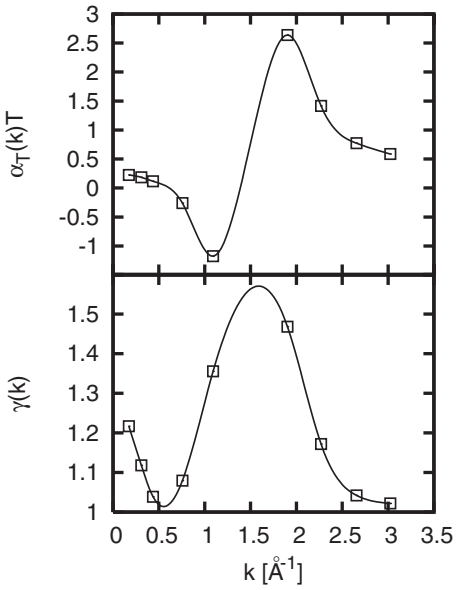

FIG. 3. Generalized wave-number-dependent ratio of specific heats $\gamma(k)$ and generalized linear thermal-expansion coefficient $\alpha_T(k)$ for molten NaI at 1080 K, obtained from classical MD simulations.

molecular-dynamics simulations. The most interesting is the behavior of $\gamma(k)$, especially its long-wavelength asymptote, which reflects the strength of coupling between thermal and viscous processes. From Fig. 3 one can estimate that the macroscopic value for the ratio of specific heats is $\gamma \approx 1.25$, which is reasonable because for molten salts the values of γ are quite close to unity like in liquid metals. Also in general the wave-number dependence of the $\gamma(k)$ is similar as for the case of liquid metals. However, the behavior of the generalized linear thermal-expansion coefficient $\alpha_T(k)$ essentially differs from the case of liquid metals. The pronounced negative peak of $\alpha_T(k)$ is an evidence of prevailed contraction in molten salt on some specific spatial scales. One should note that the pronounced negative and positive peaks in the wave-number dependence of $\alpha_T(k)$ are located on different sides of the position of the main peak of static structure factor $S_{cc}(k)$, which implies the leading role of charge fluctuations in behavior of the generalized linear thermal-expansion coefficient $\alpha_T(k)$ on the length scales compared with the nearest-neighbor distance.

B. Time-correlation functions

Time-correlation functions, derived in molecular-dynamics simulations, are the main quantities that are needed for the subsequent GCM analysis and which contain information on the wave-number dependence of different specific correlation times of the system. For the chosen basis set of six dynamical variables, which actually corresponds to the viscoelastic dynamical model, our main focus is on three partial density-density time-correlation functions. The basis set $\mathbf{A}^{(6)}(k,t)$ of the viscoelastic dynamical model provides within the GCM approach a correct reproduction of the first five frequency moments of partial dynamical structure factors for each function $F_{ij}(k,t), i=\mathrm{Na,I}$, as well as additional sum rules for the correlation times of MD-derived functions and their GCM replicas. The GCM replicas are the solutions of generalized Langevin equation, represented in six-exponential form (3), where each term corresponds to a contribution from collective eigenmode $z_\alpha(k)$, and complex weight coefficients $G_{ij}^{\alpha}(k)$ are represented via the eigenvectors associated with αth eigenmode. As it was suggested in Ref. 25 for the analysis of mode contributions it is most convenient to mark purely real eigenvalues as $d_\alpha(k)$ and switch to purely real weight coefficients instead of the complex ones. One obtains

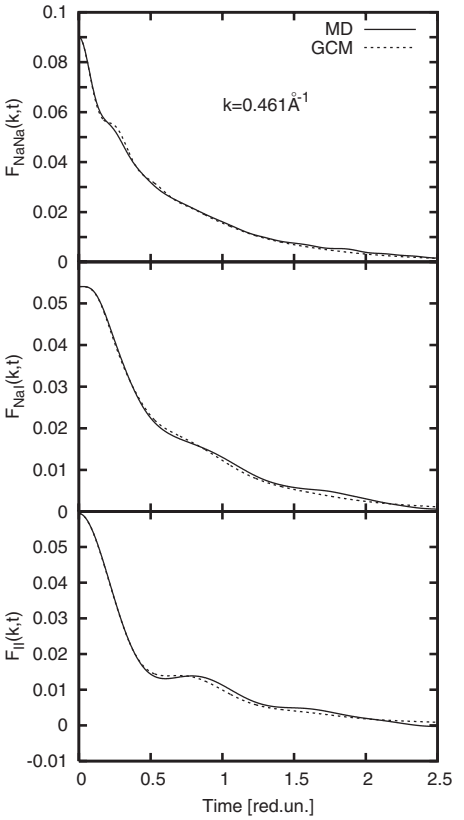

FIG. 4. Partial density-density time-correlation functions Na-Na (top), Na-I (medium), and I-I (bottom) for molten NaI at 1080 K: solid lines—AIMD simulations, dashed lines—the GCM replicas of the time-correlation functions. The time scale $\tau=0.886$ ps.

$$\frac{F_{ij}^{(6)}(k,t)}{F_{ij}(k)} = \sum_{\alpha=1}^{2} A_{ij}^{\alpha}(k) e^{-d_\alpha(k)t} + \sum_{\alpha=1}^{2} \{B_{ij}^{\alpha}(k)\cos[\omega_\alpha(k)t] + D_{ij}^{\alpha}(k)\sin[\omega_\alpha(k)t]\} e^{-\sigma_\alpha(k)t}, \quad (10)$$

with the real k-dependent amplitudes of mode contributions: from relaxation processes $A_{ij}^{\alpha}(k)$, symmetric $B_{ij}^{\alpha}(k)$ and asymmetric $D_{ij}^{\alpha}(k)$ contributions from the αth collective propagating excitation with the frequency $\omega_\alpha(k)$, and the damping $\sigma_\alpha(k)$. The quality of the GCM replicas can be seen from Fig. 4, where the MD-derived partial density-density time-correlation functions are well reproduced by six-term expression (10) and amplitudes of mode contributions from the corresponding eigenvalues are estimated without any fitting.

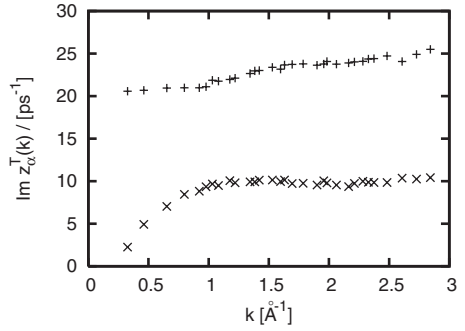

FIG. 5. Spectrum of transverse collective excitations for a liquid NaI at 1080 K, obtained within the four-variable dynamical model $\mathbf{A}^{(4T)}(k,t)$. The high- and low-frequency branches of collective excitations, shown by symbols plus and cross, correspond to the opticlike modes and shear waves, respectively.

C. Transverse and longitudinal propagating collective excitations

Transverse collective dynamics in liquids is not as complex as the longitudinal one because of absence of its coupling to thermal fluctuations and many important relaxation processes. Therefore for the estimation of transverse collective excitations one can restrict the treatment by the four-variable dynamic model $\mathbf{A}^{(4T)}(k,t)$. When the transverse correlation times

$$\tau_{ii}^T(k) = \frac{1}{C_{ii}^T(k,0)} \int_0^\infty C_{ii}^T(k,t)dt, \quad i = t,x, \tag{11}$$

are taken into account within the GCM scheme, the transverse eigenmodes are complex numbers with nonzero real part that corresponds to particular wave-number-dependent damping coefficients, which in their turn renormalize the dispersion of propagating modes. In Eq. (11) the $C_{tt}^T(k,t)$ and $C_{xx}^T(k,t)$ are the transverse total and mass-concentration current autocorrelation functions, respectively. The relaxation processes that are reflected by the transverse correlation times [Eq. (11)] are the ones connected with shear viscosity and conductivity [for $i=t$ and x in Eq. (11), respectively]. In general, there are two branches of transverse collective excitations in molten NaI: the low- and high-frequency branches correspond in the region $k<1$ Å^{-1} to the shear waves and transverse optic modes, respectively. For larger wave numbers there exists a crossover to a partial type of collective dynamics,[13] and both branches describe collective excitations mainly connected with dynamics of light (Na) and heavy (I) particles in the melt on short-range scale. In the limit $k\to 0$ according to hydrodynamics the shear waves cannot propagate in the liquid, which can be seen in Fig. 5 as a clear tendency for the low-frequency branch to reach the zero frequency approximately at $k\sim 0.25$ Å^{-1}.

The dispersion $\omega_\alpha(k)=\mathrm{Im}[z_\alpha(k)]$ and damping $\sigma_\alpha(k)=\mathrm{Re}[z_\alpha(k)]$ of longitudinal collective modes obtained within the viscoelastic model $\mathbf{A}^{(6)}(k,t)$ for the temperatures of 953 and 1080 K are shown in Fig. 6. In the long-wavelength region there exists almost linear dispersion law shown by dashed lines although the damping (real parts of complex eigenvalues) is essentially different from the hydrodynamic

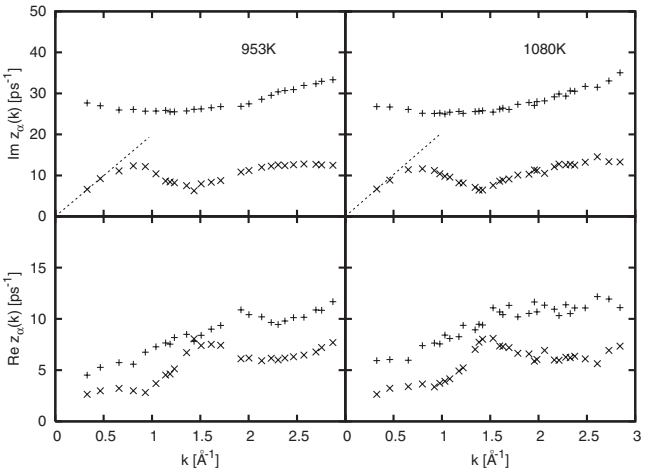

FIG. 6. Spectrum of collective excitations for a liquid NaI at 953 (right frames) and 1080 K (left frames), obtained for the dynamical model $\mathbf{A}^{(6)}(k,t)$ [Eq. (4)]. The high- and low-frequency branches, shown by symbols plus and cross, correspond to longitudinal-optic-like and acoustic excitations, respectively. The dashed lines correspond to expected linear dispersion law in the long-wavelength region. Imaginary and real parts of complex eigenvalues correspond to dispersion and damping of corresponding collective excitations.

wave-number dependence proportional to k^2. The observed tendency in k dependence of damping is close to linear in that region, which usually is observed in liquid metals beyond the hydrodynamic regime. To reach the wave numbers, where hydrodynamic behavior of damping is $\propto k^2$, much larger systems with the number of particles $N\sim 10^3$ must be simulated. Even in classical simulations with 1000 particles we were not able to reach the hydrodynamic asymptote of sound damping. We would like to remind here that the hydrodynamic regime (hydrodynamic asymptotes of main collective processes) appears only on the large spatial scales, where the liquid system is treated as continuum (no fine atomic structure). In that sense the molten salts due to screening effects have more nonuniform structure than simple liquid mixtures that is reflected in more narrow hydrodynamic region.

For longitudinal opticlike excitations the frequency and damping tend in the long-wavelength limit to nonzero values. This means that, on large spatial scales due to quite large damping of optic modes (in comparison with the damping of acoustic excitations $\propto k^2$ in this limit), they will not survive and therefore their contribution to the long-wavelength collective dynamics is negligible, as it must be for kinetic collective modes. From Fig. 6 one can estimate that the damping of acoustic and optic excitations increases with temperature, which is reasonable. Only for the region close to the main peak position of the concentration-concentration static structure factor $S_{cc}(k)$ the damping of low-frequency excitations shows a pronounced peak, which corresponds to a strong scattering of these excitations on long-lived cages of positive and negative ions. The dispersion of optic modes almost does not change with temperature. We obtained the frequency of longitudinal-optic modes at $k\to 0$ to be about 29 ps^{-1} while the transverse long-wavelength optic modes

have the frequency ~ 20.5 ps^{-1}, which means the width of propagation gap between LO and TO excitations is 8.5 ps^{-1}. In comparison with the rigid-ion simulations, where the gap between the LO and TO excitations was about 15 ps^{-1}, we obtained essential reduction in the width of the propagation gap due to electronic polarization effects.

D. Wave-number-dependent relaxation processes

Within the six-variable viscoelastic model there are two purely real eigenvalues $d_\alpha(k)$, which correspond to wave-number-dependent relaxation processes in molten NaI. In fact, there should be at least three relaxation processes affecting propagating processes in binary liquid melts: connected with heat diffusion, ionic conductivity, and structural relaxation. First two processes are the hydrodynamic ones while the structural relaxation is a nonhydrodynamic relaxation process and is important only beyond hydrodynamic regime. However, in the six-variable viscoelastic treatment the heat fluctuations are not considered in the model; hence, only two relaxation processes connected with ionic conductivity and structural relaxation represent the two real eigenvalues of the present GCM analysis. The estimated value in classical MD simulations of the ratio of specific heats means that one can expect the mode strength of thermal relaxation process in the limit $k \to 0$ to be $A^{\text{th}} \approx (\gamma - 1)/\gamma \sim 0.2$. However, our current and previous results for molten salts[19,26] point out that with increasing wave number the contribution from the thermal processes to the partial density-density time-correlation functions rapidly decays and becomes very small for $k > 0.4$ Å^{-1}, which actually justifies the applicability of the viscoelastic approximation for wave numbers larger than 0.4 Å^{-1}.

A specific feature of the molten salts is the finite lifetime of the relaxation process, connected with ionic conductivity $\tau_{\text{cond}} = d_{\text{cond}}^{-1}(k=0)$ in the long-wavelength limit, which is completely different from the well-known asymptotes for hydrodynamic relaxation processes of nonionic liquids with $d_\alpha(k) \sim k^2$.[27] The hydrodynamic expression for the relaxation process connected with ionic conductivity σ (Ref. 28),

$$d_{\text{cond}}(k) = \frac{4\pi\sigma}{\varepsilon} + O(k^2), \tag{12}$$

permits estimation of the conductivity from the long-wavelength limit of the relevant purely real eigenvalue. In Fig. 7 the wave-number dependence of two real eigenvalues for each temperature is shown. More short-time processes in long-wavelength region correspond to relaxation process Eq. (12), while in the region of sharp first peak of $S_{cc}(k)$ it has pronounced minimum and becomes the slowest relaxation process in the system on specific spatial scale. One can see that the behavior of $d_{\text{cond}}(k)$ fits very well to a quadratic k dependence according to Eq. (12). From such a fit one can estimate the values of ionic conductivity, which are: 1.05 ohm^{-1}/cm for 953 K and 1.29 ohm^{-1}/cm for 1080 K. This reflects the correct tendency of increasing conductivity with temperature; however one should note that these results were obtained within the viscoelastic treatment, which produces underestimated values of transport coefficients because

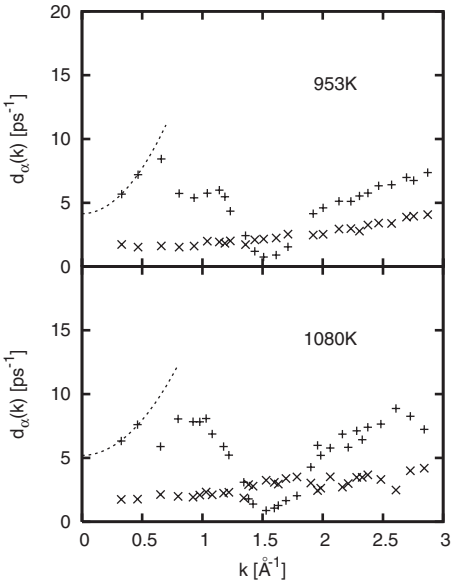

FIG. 7. Wave-number dependence of purely real eigenmodes, corresponding to inverse lifetimes of relaxation processes in molten NaI at two temperatures. The mode $d_{\text{str}}(k)$ shown by cross symbols describes the structural relaxation, while $d_{\text{cond}}(k)$ shown by plus symbols is connected with ionic conductivity. According to the hydrodynamic picture the mode $d_{\text{cond}}(k)$ tends as shown by the dashed lines in the long-wavelength limit to nonzero constant (12), proportional to ionic conductivity of the molten salt.

of the neglect of thermal processes in the model. Therefore for quantitative comparison of the obtained estimates for the ionic conductivity with experimental data, one would have to take into account corrections due to processes connected with thermal conductivity and cross correlations in the molten salts.

E. Mode contributions to the time-correlation functions

The GCM analysis of the MD-derived time-correlation functions is very useful for understanding the main contributions to different time-correlation functions in a wide region of wave numbers ranging from the hydrodynamic region up to the kinetic regime. It is very important because such an analysis can shed light on the problem of nonhydrodynamic collective processes and their manifestation in the shape of time-correlation functions and corresponding spectral functions.

The amplitudes of mode contributions $A_{ij}^{\alpha}(k)$ and $B_{ij}^{\alpha}(k)$ (sometimes called mode strengths) correspond to relaxation and propagating processes, respectively, according to Eq. (10). In Fig. 8 the total density autocorrelation functions are shown for two wave numbers in order to see the tendency in damping the oscillatory behavior in the shape of the density-density time-correlation function. It is similar to other molten salts that the contribution from acoustic propagation excitations is quite small even in the long-wavelength region although according to hydrodynamics in the long-wavelength limit their mode strength in NaI must be $\sim \gamma^{-1} = 0.8$, i.e., four times larger contribution than the one from the thermal relaxation process. It is a long-standing issue why, in the mol-

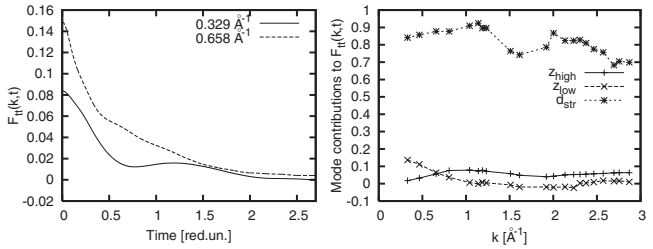

FIG. 8. Total density autocorrelation functions (left frame) for two small wave numbers, and corresponding wave-number-dependent mode contributions from the propagating modes and structural relaxation process (right frame) for molten NaI at 953 K. The contributions from the high- and low-frequency collective excitations z_{high} and z_{low} are shown by the same symbols as their dispersion in Fig. 6. The wave-number dependence of the structural relaxation process, $d_{\mathrm{str}}(k)$, is shown in Fig. 7 by cross symbols. The time scale is $\tau_\sigma = 0.934$ ps.

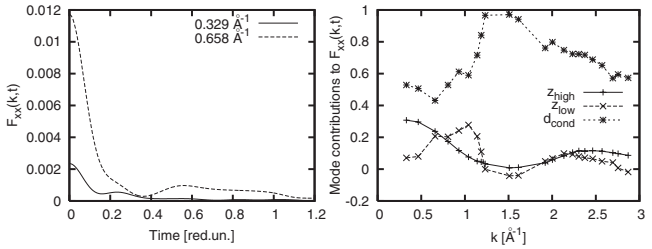

FIG. 9. Mass-concentration density autocorrelation functions (left frame) for two small wave numbers, and corresponding wave-number-dependent mode contributions from the propagating modes and leading relaxation process (right frame) for molten NaI at 953 K. The contributions from the high- and low-frequency collective excitations, z_{high} and z_{low}, are shown by the same symbols as their dispersion in Fig. 6. The wave-number dependence of the relaxation process connected with ionic conductivity $d_{\mathrm{cond}}(k)$ is shown in Fig. 7 by plus symbols. The time scale is $\tau_\sigma = 0.934$ ps.

ten salts with γ values similar as in liquid metals, the sound excitations are not well pronounced on the shape of total dynamical structure factor[29] like in liquid metals. From the right frame of Fig. 8, where the leading contributions to the total density autocorrelation functions in wide region of wave numbers are shown, one can judge that the nonhydrodynamic process of structural relaxation plays a very important role. It seems that the hydrodynamic region for molten salts is much smaller because of structural features of molten salts, where long-living cages of opposite charged ions exist, and this affects the width of the region with true hydrodynamic asymptotes. The upper bound of the hydrodynamic regime can be obtained when the relaxation times of thermodiffusive and structural modes coincide. A detailed study of wave-number dependence of structural relaxation and its contribution to collective dynamics of liquids is presented in Ref. 30.

It follows from the wave-number dependence of the mode strengths of propagating processes in Fig. 8 that the contribution from the opticlike mode vanishes toward smaller wave numbers that is the correct tendency for the kinetic collective modes. However, the contribution from the high-frequency branch to $F_{tt}(k,t)$ becomes larger than the one from the low-frequency excitations, for $k > 0.8$ Å^{-1}. This corresponds to the atomic-scale region, where the contribution of light particles to the collective dynamics prevails.

At small wave numbers the mass-concentration density autocorrelation functions also display oscillatory behavior (Fig. 9). However, the oscillations on the shape of $F_{xx}(k,t)$ are due to the high-frequency opticlike modes, which according to results of analytical treatment[26] have nonzero contributions to the normalized function $F_{xx}(k,t)/F_{xx}(k,0)$ in long-wavelength limit. For wave numbers $k > 0.7$ Å^{-1} both types of collective excitations contribute to $F_{xx}(k,t)$ although the leading contribution comes from the relaxation process connected with ionic conductivity.

F. X-ray weighted total dynamical structure factors

In order to compare our calculations with experimental dynamical structure factors, we analyze the shape of the IXS-weighted total dynamical structure factor

$$S_{\mathrm{IXS}}(k,\omega) = b_{\mathrm{Na}}^{*2}(k) c_{\mathrm{Na}} S_{\mathrm{NaNa}}(k,\omega) + 2 b_{\mathrm{Na}}^{*}(k) b_{\mathrm{I}}^{*}(k) \sqrt{c_{\mathrm{Na}} c_{\mathrm{I}}} S_{\mathrm{NaI}}(k,\omega) + b_{\mathrm{I}}^{*2}(k) c_{\mathrm{I}} S_{\mathrm{II}}(k,\omega), \quad (13)$$

where $S_{ij}(k,\omega)$ are the partial dynamic structure factors,

$$b_i^*(k) = \frac{f_i(k)}{\sqrt{c_{\mathrm{Na}} f_{\mathrm{Na}}^2(k) + c_{\mathrm{I}} f_{\mathrm{I}}^2(k)}}, \quad i = \mathrm{Na}, \mathrm{I},$$

and $f_i(k)$ are the wave-number-dependent IXS-scattering amplitudes for Na and I ions, and c_i are the concentrations, which for the NaI both are equal 0.5.

The linear combination of partial dynamic structure factors [Eq. (13)] can be used for calculations of the IXS-weighted amplitudes of mode contributions, which follow from the GCM analysis of each partial function, as it was done in Ref. 31. In Fig. 10 one can see that the contribution from the high-frequency branch in the long-wavelength region almost vanishes, and the only propagating modes contributing to the $S_{\mathrm{IXS}}(k,\omega)$ are the acoustic excitations although even they are not seen on its shape in the wave-number range studied experimentally in Ref. 10 as it is shown in Fig. 11.

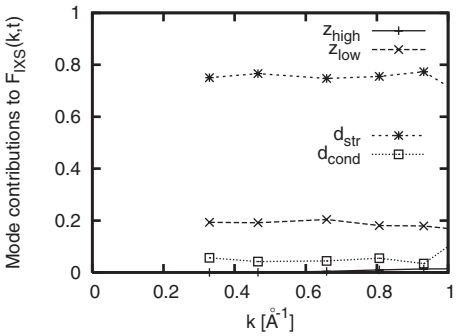

FIG. 10. Wave-number-dependent mode contributions from the propagating modes and relaxation processes to the x-ray weighted density-density time-correlation functions for molten NaI at 953 K. Notations for the collective modes are the same as in Figs. 8 and 11.

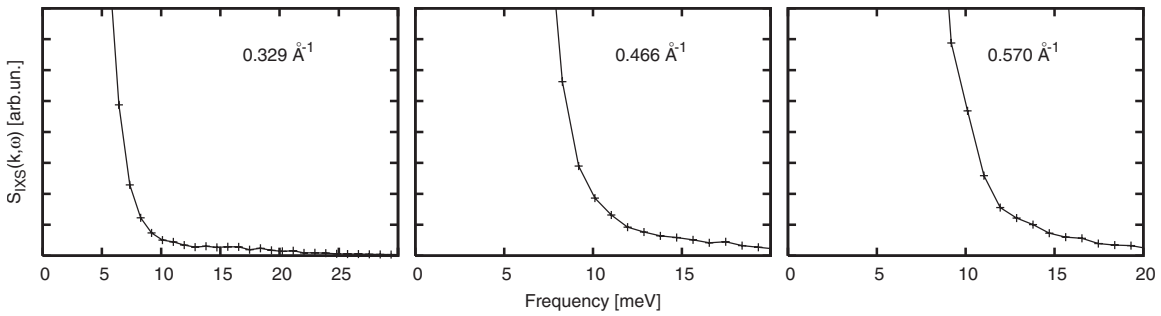

FIG. 11. X-ray weighted total dynamical structure factors for small wave numbers for molten NaI at 953 K.

Another expression for IXS-weighted scattering intensity, used in Ref. 10,

$$I_{\mathrm{IXS}}(k,\omega) \propto [f_{\mathrm{Na}}(k) + f_{\mathrm{I}}(k)]^2 S_{tt}(k,\omega) + [f_{\mathrm{Na}}^2(k) - f_{\mathrm{I}}^2(k)] S_{tq}(k,\omega) + [f_{\mathrm{Na}}(k) - f_{\mathrm{I}}(k)]^2 S_{qq}(k,\omega), \quad (14)$$

can be analyzed from the point of view of wave-number-dependent amplitudes shown in Figs. 8 and 9. One of the arguments of expectation to observe optic modes in Ref. 10 was a suggestion that there can be quite strong contribution from the charge-charge dynamic structure factor $S_{qq}(k,\omega)$ to the total IXS-weighted intensity. However, Fig. 9 makes evidence that the optic modes really have nonvanishing contribution to the *normalized* dynamic structure factor

$$S_{qq}(k,\omega)/S_{qq}(k) \sim S_{xx}(k,\omega)/S_{xx}(k),$$

while the static structure factor $S_{xx}(k)$ vanishes as k^2 in the long-wavelength region and therefore the contribution from optic modes to the shape of $S_{qq}(k,\omega)$ and $I_{\mathrm{IXS}}(k,\omega)$ vanishes also as k^2. This excludes practically the possibility of observation of optic modes in molten salts for small wave numbers $k < 0.8$ Å^{-1} in the scattering experiments.

IV. CONCLUSIONS

We performed an *ab initio* study of dispersion and damping of collective modes in molten NaI at two temperatures. The theoretical approach used in this study consists in estimation of dynamical eigenmodes, which contribute with different weights to the time-correlation functions, obtained in *ab initio* molecular dynamics. These weights (or mode strengths) clearly reflect the contributions of acoustic and optic collective excitations to different spectral functions as well as to the experimental IXS intensities. The two main messages of our study are:

(i) Our *ab initio* simulations in combination with the parameter-free GCM approach predict the frequency window 25–35 ps^{-1} for the high-frequency branch of collective excitations in molten NaI in a temperature range up to 1080 K. The long-wavelength longitudinal-optic modes have the frequency 29 ps^{-1} while the transverse optic modes at $k \to 0$ are separated from the longitudinal modes by a gap of 8.5 ps^{-1}.

(ii) The analysis of mode contributions reveals the absence of contribution from opticlike excitations to the total dynamical structure factor in the long-wavelength region that is in complete agreement with the theory of nonhydrodynamic optic modes in liquids.[13,14] The calculated IXS-weighted dynamical structure factor of molten NaI at 953 K shows no side peak due to the optic modes in the region $k < 0.8$ Å^{-1} that does not support the reported possible observation of optic modes in molten NaI.[10]

ACKNOWLEDGMENTS

This study was supported in part by the State Foundation for Fundamental Research of Ukraine under Contract No. Ф28.2/038 and by the National Academy of Sciences of Ukraine. The calculations have been performed using the *ab initio* total-energy and molecular-dynamics program VASP (Vienna *ab initio* simulation package) developed at the Institute für Materialphysik of the Universität Wien.[32–34] The allocation time at the Supercomputer Center of National Technical University of Kiev is acknowledged.

[1] T. Scopigno, G. Ruocco, and F. Sette, Rev. Mod. Phys. **77**, 881 (2005).
[2] Ya. Chushak, T. Bryk, A. Baumketner, G. Kahl, and J. Hafner, Phys. Chem. Liq. **32**, 87 (1996).
[3] N. Anento, L. E. Gonzalez, D. J. Gonzalez, Ya. Chushak, and A. Baumketner, Phys. Rev. E **70**, 041201 (2004).
[4] N. H. March and M. P. Tosi, *Coulomb Liquids* (Academic, NewYork, 1984).
[5] M. Dixon, Philos. Mag. B **47**, 531 (1983).
[6] O. Alcaraz and J. Trullas, J. Mol. Liq. **136**, 227 (2007).
[7] O. Alcaraz, V. Bitrian, and J. Trullas, J. Chem. Phys. **127**, 154508 (2007).
[8] N. Galamba and B. J. Costa Cabral, J. Chem. Phys. **127**, 094506 (2007).
[9] K. Parlinski, J. Phys.: Conf. Ser. **92**, 012009 (2007).
[10] F. Demmel, S. Hosokawa, W.-C. Pilgrim, and S. Tsutsui, Nucl. Instrum. Methods Phys. Res. B **238**, 98 (2005).
[11] I. M. de Schepper, E. G. D. Cohen, C. Bruin, J. C. van Rijs, W.

Montfrooij, and L. A. de Graaf, Phys. Rev. A **38**, 271 (1988).
[12] T. Bryk, I. Mryglod, and G. Kahl, Phys. Rev. E **56**, 2903 (1997).
[13] T. Bryk and I. Mryglod, J. Phys.: Condens. Matter **12**, 6063 (2000).
[14] T. Bryk and I. Mryglod, J. Phys.: Condens. Matter **14**, L445 (2002).
[15] I. M. Mryglod, Condens. Matter Phys. **1**, 753 (1998).
[16] A. B. Bhatia, D. E. Thornton and N. H. March. Phys. Chem. Liq. **4**, 97 (1974).
[17] J. Hafner, J. Phys. C **16**, 5773 (1983).
[18] T. Bryk and I. Mryglod, Chem. Phys. Lett. **466**, 56 (2008).
[19] T. Bryk and I. Mryglod, Phys. Rev. B **71**, 132202 (2005).
[20] G. Kresse and J. Hafner, J. Phys.: Condens. Matter **6**, 8245 (1994).
[21] J. P. Perdew and Y. Wang, Phys. Rev. B **45**, 13244 (1992).
[22] C. Ciccotti, G. Jacucci, and I. R. McDonald, Phys. Rev. A **13**, 426 (1976).
[23] M. Revere and M. P. Tosi, Rep. Prog. Phys. **49**, 1001 (1986).
[24] T. Bryk and I. Mryglod, J. Phys.: Condens. Matter **17**, 413 (2005).
[25] T. Bryk and I. Mryglod, Phys. Rev. E **64**, 032202 (2001).
[26] T. Bryk and I. Mryglod, J. Phys.: Condens. Matter **16**, L463 (2004).
[27] J.-P. Hansen and I. R. McDonald, *Theory of Simple Liquids* (Academic, London, 1986).
[28] P. V. Giaquinta, M. Parrinello, and M. P. Tosi, Phys. Chem. Liq. **5**, 305 (1976).
[29] J.-B. Suck, J. Neutron Res. **14**, 317 (2006).
[30] T. Bryk and I. Mryglod, Condens. Matter Phys. **11**, 139 (2008).
[31] S. Cazzato, T. Scopigno, T. Bryk, I. Mryglod, and G. Ruocco, Phys. Rev. B **77**, 094204 (2008).
[32] G. Kresse and J. Hafner, Phys. Rev. B **47**, 558 (1993); **49**, 14251 (1994).
[33] G. Kresse and J. Furthmüller, Comput. Mater. Sci. **6**, 15 (1996).
[34] G. Kresse and J. Furthmüller, Phys. Rev. B **54**, 11169 (1996).